Optica Applicata, Vol. XII, No. 2, 1982

Diffraction images of two dimensional elliptical objects

AMI CHANDRA, R. N. SINGH, K. SINGH

Physics Department, Indian Institute of Technology, Delhi, New Delhi-110016, India.

This paper is devoted to a theoretical study of the diffraction images of elliptical objects formed by the ideal systems having circular and angular apertures. The object illumination is assumed to be incoherent. Intensity distribution in the images has been evaluated by using the Fourier transformation approach. Results have been presented in the form of graphs along two directions in the image plane.

1. Introduction

The importance of imagery of isolation extended objects in the performance evaluation of an optical system such as in aerial photography is now well-known. When the system being tested is asymmetrical, it is desirable to measure the resolution in the specific directions. In this connection, it is important to investigate the diffraction images of two dimensional objects such as the disk and annulus, etc. A critical analysis of different targets used in various countries for determining the resolution of the optical system is given by ARTISHEVSKII and GRADOBOEV [1].

Diffraction images of the disk formed by an aberration free as well as by a defocused system were studied by WEINSTEIN [2], while BARAKAT and HOUSTON [3] investigated the effect of symmetric aberrations. Motion afflicted images of the disk were studied by RATTAN and SINGH [4]. Gupta and Singh studied the diffraction images of disk objects in the presence of astigmatism. GUPTA et al. [6] investigated the influence of optimum balanced coma on the disk spread function and a list of references concerning the work in this direction can be found there.

Elliptical objects are also important in the fine particle science where the shape of a particle is often compared to its equivalent, rectangular or elliptical objects [7,8]. The diffraction pattern sampling can be used to characterize the shape of a particle. It is well known that the object and its Fraunhofer diffraction pattern form a Fourier transform pair under certain circumstances. Now the Fraunhofer diffraction pattern of an object is related to the shape, size and orientation of the object. Hence, the diffraction pattern of an object can be used to describe the object [9].

An increasing use of annular aperture systems in space optics [10], night vision aids [11], low light level systems [12] and optical processing of degraded images [13] has generated a renewed interest in the study of the properties of the images formed by annular aperture systems. OTTERMAN [14] discussed the

problem of imaging a geoscene formed by such systems. MEKLER et al. [15] studied various aspects of diffraction effects such as irradiance distribution, resolution and size estimation in diffraction limited imagery of extended circular and annular apertures. Some of the recent studies in this connection are due to MANGUS and UNDERWOOD [16], PRICE and WINTER [17], POWELL [18, 19], TSCHUNKO [20, 21] and MAHAJAN [22].

In view of what has been said above, we have studied theoretically the diffraction images of elliptical objects formed by the diffraction limited optical systems having circular aperture with and without obstruction in the pupil.

2. Theory

2.1. Fourier spectrum of the object

Let the equation of the ellipse be

$$\frac{x'^2}{a^2}+\frac{y'^2}{b^2}=1, \tag{1}$$

which is reduced to the standard equation of the circle by the transformation of variables as $x'=ax$ and $y'=by$. Now, the transmittance of intensity in an incoherently illuminated object can be represented as

$$f(x,y)=\begin{cases}1.0 & \text{for } x^2+y^2\leqslant 1,\\ 0.0 & \text{otherwise.}\end{cases} \tag{2}$$

The spatial frequency spectrum of such an object is the two dimensional Fourier transform of the object intensity distribution. Accordingly,

$$\begin{aligned} O(p,q) &= \int_{-\infty}^{\infty}\int f(x',y')\exp\{-2\pi i(px'+qy')\}\,dx'\,dy' \\ &= ab\int_{-\infty}^{\infty}\int f(x,y)\exp\{-2\pi\, i\,(pax+qby)\}\,dx\,dy. \end{aligned} \tag{3}$$

On substituting (2) for $f(x,y)$ and integrating, one obtains

$$O(p,q)=\frac{a}{\pi q}\int_{-1}^{1}\exp(-2\pi iaxp)\sin(2\pi bq\sqrt{1-x^2})\,dx. \tag{4}$$

The above integral can be written as the sum of real and imaginary parts. The imaginary part, being an odd function of x, vanishes on integration. The object spectrum can now be written as

$$O(p,q)=\frac{2a}{\pi q}\int_{0}^{1}\cos(2\pi apx)\sin(2\pi bq\sqrt{1-x^2})\,dx. \tag{5}$$

Using the integral due to GRADSHTEYN and RYZHIK [23] it is reduced to

$$O(p, q) = 2\pi ab J_1(a^2p^2+b^2q^2)^{1/2}/(a^2p^2+b^2q^2)^{1/2}, \tag{6}$$

(J_1 — Bessel function of first kind). By changing the frequency variables (p, q) to the polar coordinates by the substitution of $p = \omega\cos\theta$ and $q = \omega\sin\theta$ (PAPOULIS [24]) equation (6) gives

$$O(\omega, \theta) = 2\pi ab\, J_1(\omega\sqrt{a^2\cos^2\theta+b^2\sin^2\theta})/(\omega\sqrt{a^2\cos^2\theta+b^2\sin^2\theta}), \tag{7}$$

where a and b are expressed in the reduced units and are related to their geometrical distances by the equations $a = \pi x/\lambda F$ and $b = \pi y/\lambda F$. The dimensionless spatial frequency ω is given by $\omega = 2k\lambda F$, where k is the spatial frequency in lines per mm, λ is the wavelength of light and F is the f-number of the optical system. The expression (7) is reduced to the well-known object spectrum, $J_1(a\omega)/a\omega$ for the circularly symmetric disk object on substituting $b = a$.

3. Intensity distribution in the diffraction image

The spatial frequency spectra of the image and object are related by the transfer function of an optical system, i.e.

$$I(\omega, \theta) = O(\omega, \theta)T(\omega, \theta). \tag{8}$$

The intensity distribution is the two dimensional inverse Fourier transform of $I(\omega, \theta)$. Therefore

$$I(v, \Phi) = \frac{1}{2\pi}\int_0^2\int_0^{2\pi} O(\omega, \theta)T(\omega, \theta)\exp\{iv\omega\cos(\theta-\Phi)\}\,\omega d\omega d\theta. \tag{9}$$

For an ideal optical system $T(\omega, \theta)$ is real and independent of θ. As the intensity is a real quantity, on taking the real part of the equation (9) (imaginary part, being the odd function of ω, will vanish on integration), the expression for intensity can be written in the following form

$$I(v, \Phi) = \frac{1}{2\pi}\int_0^2\int_0^{2\pi} O(\omega, \theta)T(\omega)\cos\{v\omega\cos(\theta-\Phi)\}\omega d\omega d\theta. \tag{10}$$

The optical transfer function for a circular aperture system is well-known

$$T(\omega) = \frac{2}{\pi}\left\{\cos^{-1}\frac{\omega}{2}-\frac{\omega}{2}\left(1-\frac{2}{4}\right)^{1/2}\right\}. \tag{11}$$

while for an annular aperture system it was given by STEEL [25] and O'NEILL [26]. For the sake of convenience it is reproduced below

$$T(\omega) = \frac{1}{(1-\eta^2)}[A+B+C], \tag{12}$$

where

$$A = \frac{2}{\pi}\left[\cos^{-1}\frac{\omega}{2} - \frac{\omega}{2}\left(1-\frac{2}{4}\right)^{1/2}\right], \text{ for } 0 \leqslant \omega/2 < 1,$$

$$A = 0, \text{ for } \omega/2 \geqslant 1,$$

$$B = \frac{2\eta^2}{\pi}\left[\cos^{-1}\frac{\omega}{2\eta} - \frac{\omega}{2\eta}\left(1-\frac{\omega^2}{4\eta^2}\right)\right]^{1/2}, \text{ for } 0 \leqslant \omega/2\eta < 1,$$

$$B = 0, \text{ for } \omega/2\,\eta \geqslant 1,$$

$$C = -2\eta^2, \text{ for } 0 \leqslant \omega/2 < (1-\eta)/2,$$

$$C = -2\eta^2 + \frac{2\eta}{\pi}\sin\Phi' + \frac{(1+\eta^2)}{\pi}\Phi' - \frac{2}{\pi}(1-\eta^2)\tan^{-1}\left[\left(\frac{1+\eta}{1-\eta}\right)\tan\frac{\Phi'}{2}\right],$$

for $(1-\eta)/2 \leqslant \omega/2 < (1+\eta)/2$,

$$C = 0, \text{ for } \omega/2 \geqslant (1+\eta)/2,$$

here $\Phi' = \cos^{-1}\left(\frac{1+\eta^2-\omega^2}{2\eta}\right)$, (and η is the obscuration ratio, i.e., the ratio between the radius of obscuration and the radius of aperture).

4. Results and discussion

The intensity distribution in the diffraction image of an incoherently illuminated elliptical object was evaluated (by using equation (10)), numerically on a high speed electronic computer ICL-2960 with the help of the Gauss-quadrature method using 40-Gauss points. In the evaluation of such integrals the accuracy of computation plays a very important role. Recently, both merits and demerits of various computational schemes for obtaining high degree of accuracy in the numerical evaluation of integrals for any combinations of functions/integrals were discussed by BARAKAT [27].

The results for various values of eccentricity of the ellipse were obtained in the case of the obscured as well as unobscured circular pupil. Our results for a perfectly circular disk object agree with those given in previous works (WEINSTEIN [2], and BARAKAT and HOUSTON [3]) for circular aperture system and with those of MELKER et al. [15] for annular aperture systems. In the limiting case of a point source, these results agree with those published by RATTAN et al. [28] and in the case of a thin line, with those of GUPTA and SINGH [29]. As the intensity distribution is not circularly symmetric, we calculated the results in two azimuthal directions, i.e., along $\Phi = 0.0$, and $\Phi = \pi/2$. The values of the obscuration ratio η (i.e., $\eta = 0.0$, 0.25, and 0.50) were considered.

Figures 1–4 show the intensity distribution in the image with different values of a and b. Figure 5 presents the line spread function for an annular

aperture system with $\eta = 0.25$ and 0.50. Figure 6 shows the variation of intensity along $\Phi = 0.0$. It may be noted that this variation is due to the finite (though very large) dimension of the object in the x-direction. Figure 7 shows the variation in central intensity as a function of the obscuration ratio η.

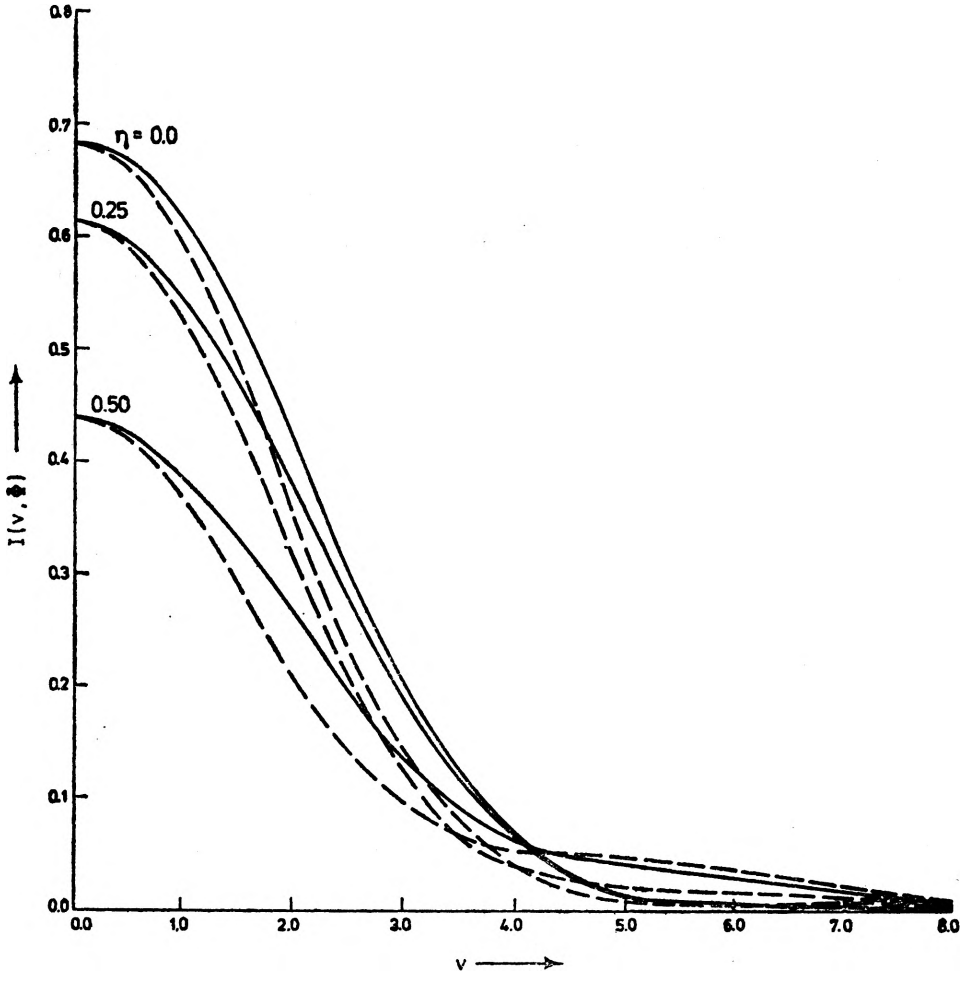

Fig. 1. Intensity distribution in the images of elliptical object with $a = 2.5$ and $b = 2.0$ $\eta = 0.0$, 0.25 and 0.50 (—— along $\Phi = 0.0$, — — — along $\Phi = \pi/2$)

Most of the results are self-explanatory. However, the important points of our investigation can be summarized as follows:

1. As was expected, the intensity in the direction along the major axis of ellipse in the region of the geometrical image is greater than that along the minor axis, which, however, seems no longer valid as we go far away from the region of the geometrical image.

2. Central intensity increases with the increasing size of the object. However, such an increase in the central intensity is comparatively smaller for the large-size objects.

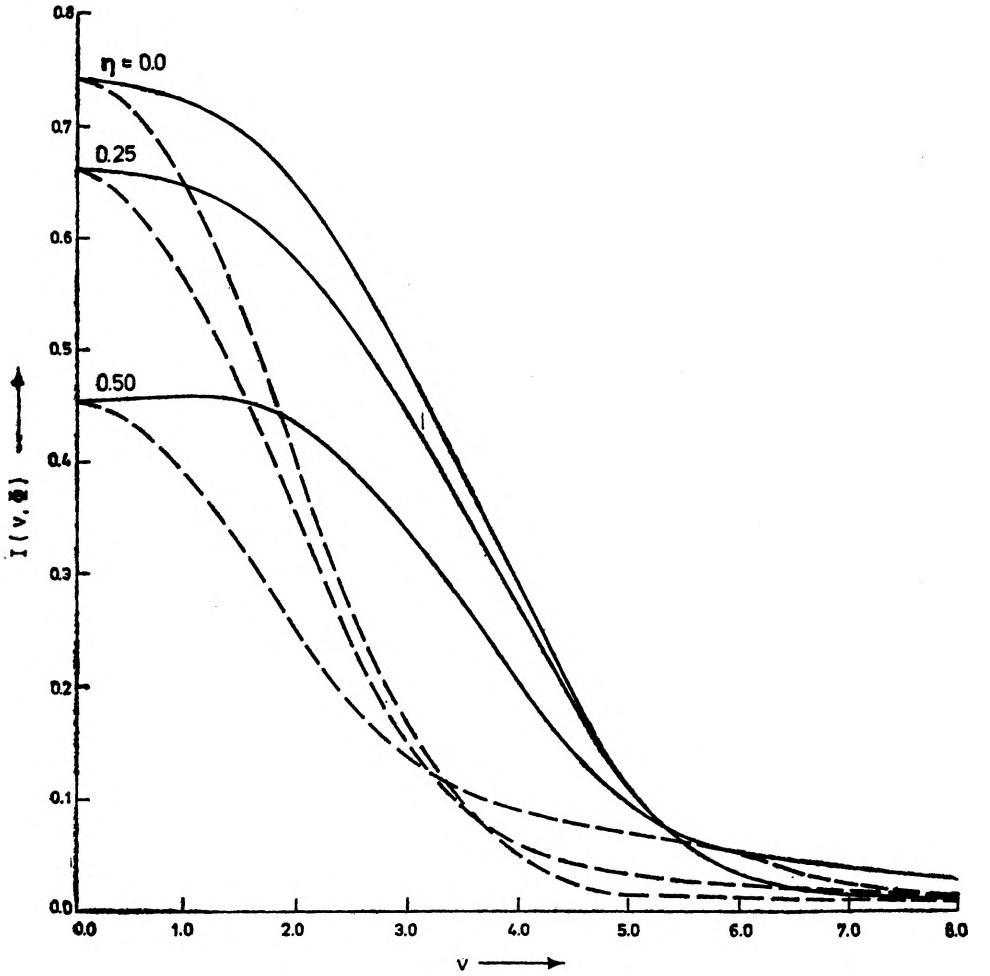

Fig. 2. The same as in Fig. 1, $a = 4.0$, $b = 2{,}0$

3. The effect of pupil obscuration is the reduction of the central intensity. More and more energy spills over the region of the geometrical image with an increase in the value of η. The intensity in the region near the geometrical image is greater along the major axis than that along the minor axis of ellipse for the small amount of pupil obscuration. However, with the increasing amount of pupil obscuration and the size of the object, the intensity along the minor axis (i.e., along $\Phi = \pi/2$) increases initially up to a certain distance from the centre within the region of the geometrical image, while its value is lower than

that of intensity along the major axis as we go away from the central region of the image. The effect is quite distinct when $\eta = 0.5$, $a = 5.0$ and $b = 4.0$ (Fig. 3). In this case, the orientation of the object may be wrongly interpreted because

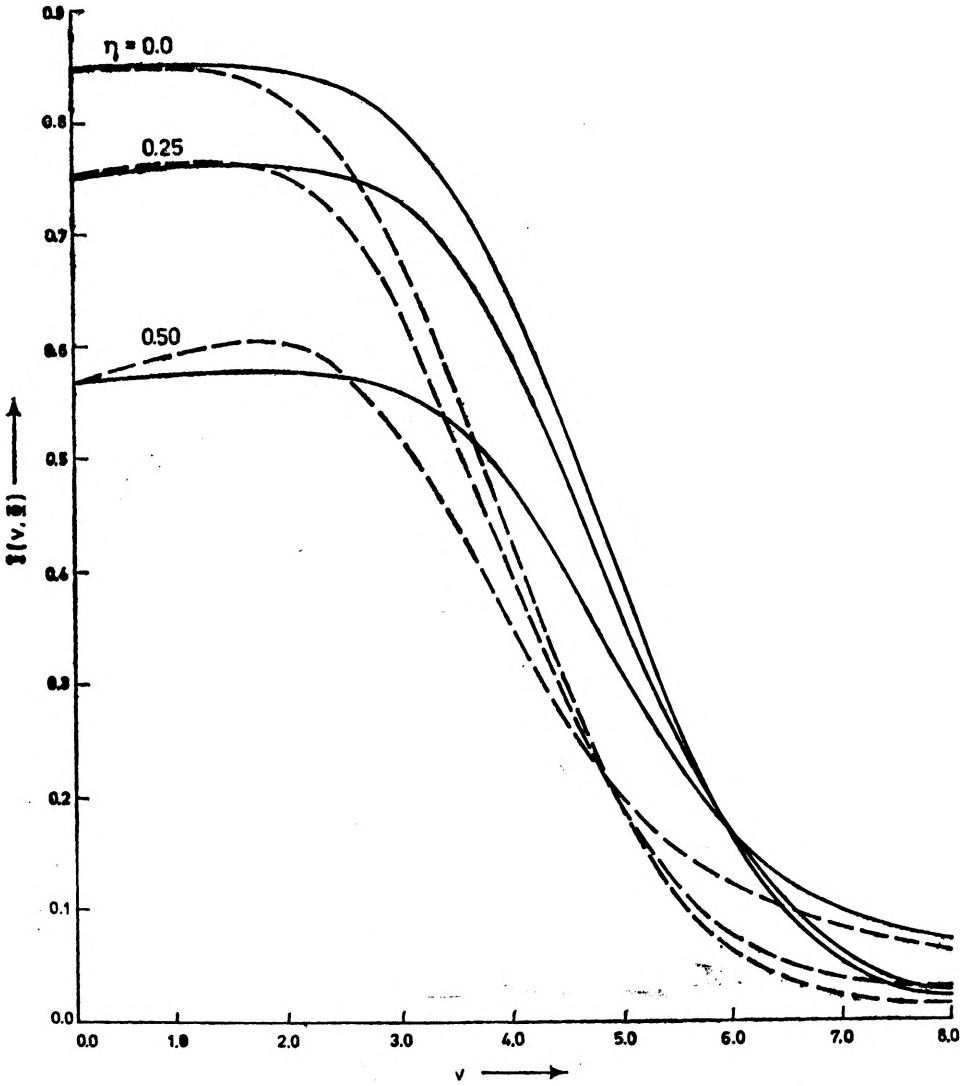

Fig. 3. The same as in Fig. 1, $a = 5.0$, $b = 4.0$

the intensity along the major axis is appreciably lower than that along the minor axis. It was observed that for $a = 5.0$ and $b = 4.0$ the maximum intensity does not occur at the centre but is displaced from the centre. This is in agreement with the results of SMITH and OSTERBERG [30] in the case of the disk image.

4. The intensity at the edge of the geometrical image is not half the central intensity in the two directions as is the case for circular targets like the disk.

The intensity is slightly lower along the major axis and slightly higher along the minor axis at the edge of the geometrical image. As can be inferred from Fig. 3, the intensity along $\Phi = 0.0$ at $v = 5.0$ is 0.38, while along the minor axis at $v = 5.0$, its value is lower. However, at $v = 4.0$ the value of intensity is 0.42 which is slightly higher than its value at the geometrical edge of the image along $\Phi = 0.0$.

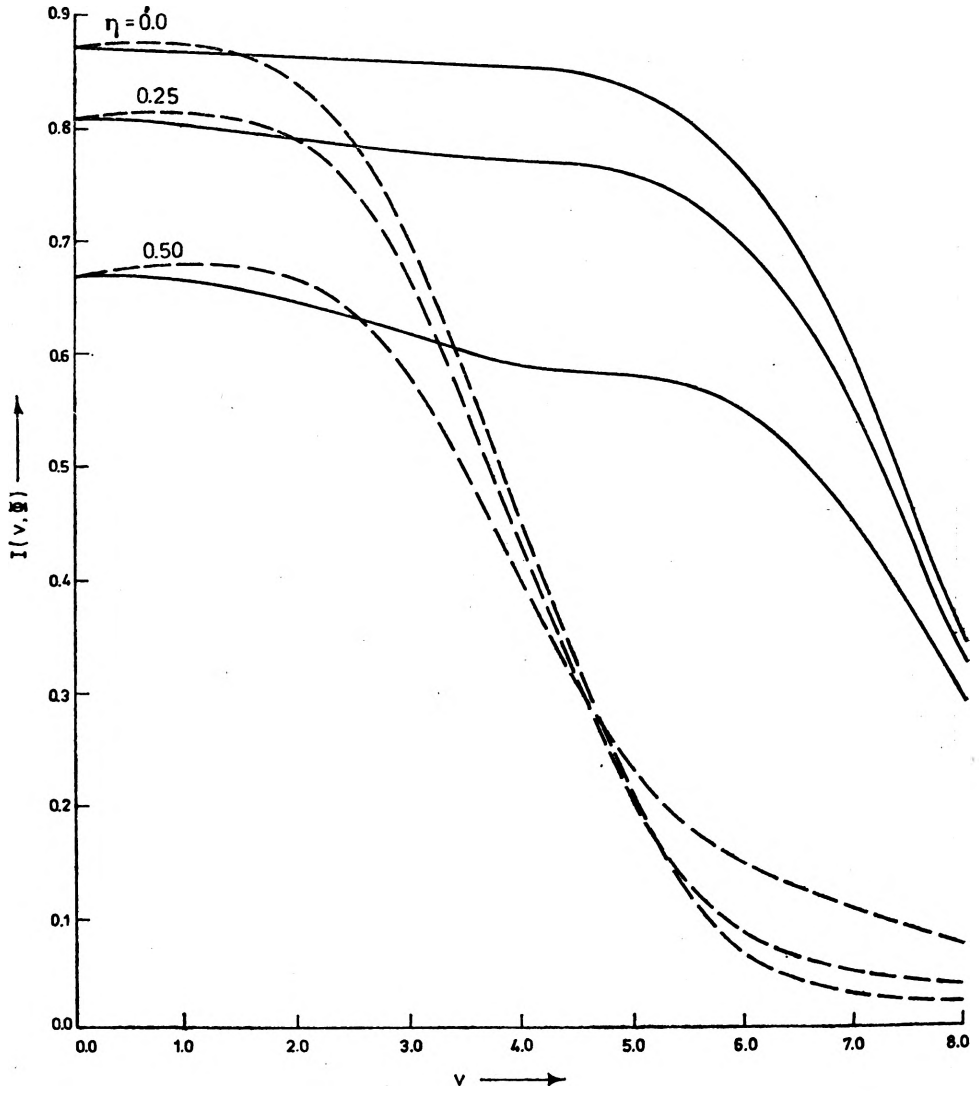

Fig. 4. The same as in Fig. 1, $a = 8.0$, $b = 4.0$

5. The slope of the intensity curve is greater along the minor axis which shows that the intensity decreases quickly along the minor axis, this decrease being slow along the major axis of the ellipse.

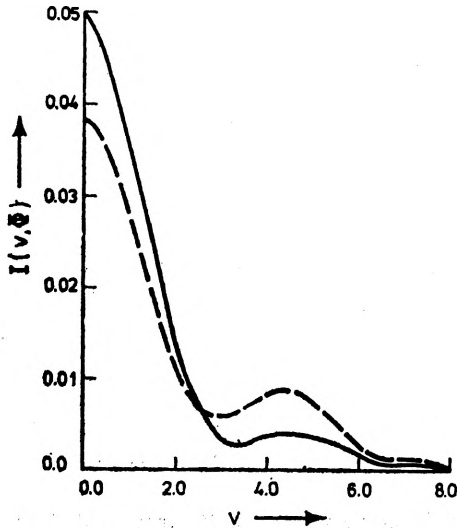

Fig. 5. Line spread function $\eta = 0.25$ (—) and 0.50 (— — —), $a = 10.0$, $b = 0.1$, $\Phi = \pi/2$

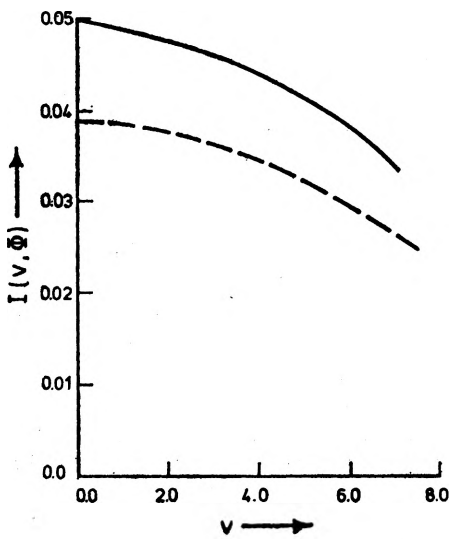

Fig. 6. Intensity variation along $\Phi = 0.0$, $a = 10.0$, b = 0.1, ———— for $\eta = 0.25$, — — — for $\eta = 0.50$

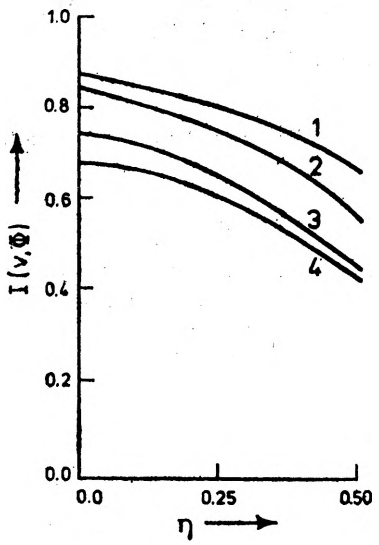

Fig. 7. Central intensity vs. obscuration ratio: 1. $a = 8.0$, $b = 4.0$, 2. $a = 5.0$, $b = 4.0$, 3. $a = 4.0$, $b = 2.0$, 4. $a = 2.5$, $b = 2.0$

References

[1] Artishevskii V.I., Gradoboev V.M., Soviet. J. Opt. Tech. **42** (1975), 672.
[2] Weinstein W., J. Opt. Soc. Am. **45** (1955), 1006.
[3] Barakat R., Houston A., J. Opt. Soc. Am. **55** (1965), 881.
[4] Rattan R., Singh K., Nouv. Rev. d'Opt. **7** (1976), 259.
[5] Gupta A.K., Singh K., Can. J. Phys. **56** (1978), 1539.
[6] Gupta A.K., Singh R.N., Singh K., ibidem, p. 12.

[7] HEYWOOD H.J., Pharm. and Pharmacol 1963, 15.
[8] HAUSER H.H., *Proc. of Conf. Soc. Annal. Ch. Particle Size Analysis*, 1966.
[9] REDMAN J.D., REID C.D., British Nucl. Energy Soc. (1967), 8.
[10] CAMERON R.M., BADER M., MOBLEY R.E., Appl. Opt. **10** (1971), 2011.
[11] AMON M., Appl. Opt. **10** (1971), 490.
[12] BECKER J., Opt. Acta **17** (1970), 481.
[13] MCCRICKERD J.T., Appl. Opt. **10** (1971), 2276.
[14] OTTERMAN J., Appl. Opt. **8** (1969), 1887.
[15] MEKLER Y., OTTERMAN J., RENVOY Z., Appl. Opt. **14** (1975), 503.
[16] MANGUS J.P., UNDERWOOD J.H., Appl. Opt. **8** (1969), 45.
[17] PRICE M.J., WINTER B., Appl. Opt. **12** (1973), 2716.
[18] POWELL I., Opt. Acta **20** (1973), 879.
[19] POWELL I., Opt. Acta **21** (1974), 453.
[20] TSCHUNKO H.F.A., Appl. Opt. **13** (1974), 22.
[21] TSCHUNKO H.F.A., ibidem **17** (1978), 1075.
[22] MAHAJAN V.N., Appl.Opt. **17** (1978), 964.
[23] GRADSHTEYN I.S,, RYZHIK I.M., *Tables for Integrals, Series and Products*, Academic Press, New York, London 1965, 399.
[24] PAPOULIS A., *Systems and Transforms with Applications in Optics*, McGraw-Hill Book. Co., 1968, 95.
[25] STEEL W.H., Rev.Opt. **32** (1953), 143.
[26] O'NEILL E.L., J.Opt. Soc. Am. **46** (1956), 285.
[27] BARAKAT R. [in] *The Computers in Optical Reserach*, Ed. B.R. Frieden, Springer-Verlag, 1980.
[28] RATTAN R., SINGH K., CHANDRA A., Ind. J. Pure and Appl. Phys. **13** (1975), 620.
[29] GUPTA A.K., SINGH K., Photogram Eng. and Remote Sensing **42** (1976), 529.
[30] SMITH L.W., OSTERBERG H., J. Opt. Soc. Am. **51** (1961), 412.

Received September 3, 1981

Дифракционное изображение двухмерных эллиптических предметов

Работа посвящена теоретическим дифракционным изображениям эллиптических предметов, созданных идеальными системами с круговыми или кольцевыми апертурами. Принято, что некогерентное освещение предметов в изображении было оценено при применении преобразования Фурье. Результаты представлены в виде графиков вдоль двух направлений в плоскости изображения.